Simulation of Fractional Brownian Motion with Micropulses

Mine Çağlar[1]
Bellcore[2], MCC
Morristown, NJ 07960, USA
mcaglar@princeton.edu

Abstract: The fractional Brownian motion traffic model efficiently captures long-range dependence and self-similarity indicated by recent measurements from a variety of packet networks. In this paper, we devise a fast and accurate algorithm of $O(n)$ for synthesizing a fractional Brownian motion, based on a recent micropulses approximation of Cioczek-Georges and Mandelbrot. Such an algorithm would be useful for further performance analysis of packet networks through simulation. After computing the numerical errors explicitly, we run simulations to illustrate the accuracy of the method. We apply wavelet estimation for statistical confirmation, and study the estimator of the peakedness parameter empirically.
Key Words: Fractional Brownian motion, fractional Gaussian noise, packet traffic, wavelet estimation.

1 Introduction

Recent measurements from a variety of packet networks indicate that aggregate packet traffic is *self-similar* (i.e., looks the same when measured over a wide range of time scales) and *long-range dependent* (i.e., correlation remains significant across arbitrarily large time lags) (MEIER-HELLSTERN et.al. (1991), DUFFY et.al. (1994), LELAND et.al. (1994), BERAN et.al. (1995), PAXON and FLOYD (1995), CROVELLA and BESTAVROS (1996)). Representation of these phenomena in the traffic model is crucial for accurate performance analysis, and in turn for traffic engineering.

[1]Current address: Koc University, Istinye 80860, Istanbul Turkey
[2]Current name: Telcordia Technologies

There exist several self-similar stochastic processes that can incorporate long-range dependence for modeling packet arrivals (SAMORODNITSKY and TAQQU (1994)). A parsimonious and compact model is the Gaussian self-similar process called *fractional Brownian motion* (FBM). In this case, the only parameters to be estimated are the mean, the variance and the Hurst parameter, which denotes the degree of self-similarity. In teletraffic studies, the autocorrelation function is the most used statistic for checking self-similarity and it is also definitive for long-range dependence. A Gaussian model is the simplest choice when only second order properties are considered as in this case. Moreover, Gaussian distribution appears naturally in highly aggregated traffic from several sources (see for example PAXON and FLOYD (1995)). In this study, we focus on the FBM traffic model with such applications in mind. For less aggregated traffic, LELAND et.al. (1994) suggest asymptotically self-similar models, and in the cases where short-range dependence exists along with long-range dependence, another self-similar model called fractional ARIMA process is more appropriate.

Empirical studies have shown that the queue performance in the presence of long-range dependence can be much different than that predicted by traditional models. The packet traffic engineering such as buffer sizing, admission control, and congestion control have to be done accordingly (e.g. FOWLER and LELAND (1991), LELAND et.al. (1994), ERAMILLI et.al. (1996)). In contrast to traditional Markovian traffic models, there exist few analytical queuing results for FBM and other self-similar models. In particular, NORROS (1995) computes the tail distribution of queue length process with FBM traffic input, and HEATH et.al. (1998) compute the same performance measure for an asymptotically self-similar model. Hence, simulation studies become crucial for further understanding of the queuing issues and generation of synthetic traces of data has attracted great research interest in the past few years (e.g. LAU et.al. (1995), PAXSON (1997)). For capturing the features of long-range dependence and for the reliability of the conclusions drawn on network performance, these traces have to be generated in long sequences fast and accurately.

In this paper, we devise a fast and accurate algorithm for generating an FBM process. The algorithm is based on a recent approximation of CIOCZEK-GEORGES and MANDELBROT (1996) through micropulses, and its complexity is only $O(n)$ where n denotes the number of sample points obtained. The approximating process is i) self-similar, ii) has stationary increments, iii) has the same autocorrelation structure as FBM, and finally, iv) its distribution, which is effectively

Gaussian for computational purposes, can be made arbitrarily close to Gaussian. Here, we compute the exact errors arising from the numerical implementation and discuss other computational issues. The new values are generated "on the fly" with no need to store the whole time series till the end of the simulation. Hence, using this algorithm, high quality traces can be generated conveniently with little computational cost using this algorithm.

The organization of the paper is as follows. In Section 2, we state the formal definitions related to FBM traffic and review the existing methods of synthesis in comparison to the proposed algorithm. In Section 3, we outline the theoretical approximation of FBM with micropulses. In Section 4, the numerical implementation of this approach is analyzed in detail and the algorithm is developed step by step. We turn to the issue of evaluation of the sample traces with wavelet analysis in Section 5. There are two purposes of this evaluation: i) establish a guide to exact choice of parameters of the micropulses approach through simulations while confirming its accuracy ii) study the estimation of the variance parameter of the FBM traffic model empirically.

2 Preliminaries and Existing Methods

In this section, we define the FBM traffic model and review the existing methods to synthesize an FBM. We also outline the proposed algorithm of micropulses in comparison to these methods.

2.1 Preliminaries

Let $A(t)$ denote the total amount of traffic (in bits, say) offered to the network in the time interval $[0, t]$. We assume that the increments of A are stationary, that is, the distribution of the increment process $\{A(t+s) - A(s) : t \geq 0\}$ is independent of s for every $s \geq 0$.

The process $A \equiv \{A(t) : t \geq 0\}$ is said to be *second-order self-similar* with Hurst parameter H if the autocorrelation functions of $\{A(\alpha t) : t \geq 0\}$ and $\{\alpha^H A(t) : t \geq 0\}$ are identical for all $\alpha > 0$. In particular, for each $t \geq 0$, the relation

$$Var(A(\alpha t)) = Var(\alpha^H A(t)) = \alpha^{2H} Var(A(t))$$

holds. In other words, in the presence of self-similarity, a scaling in time is compensated by an appropriate scaling in space.

Let $r(k)$ denote the autocovariance function of the increments of A at integer times. That is, $r(k) = Cov(A(k+1) - A(k), A(1) - A(0))$ for $k = 0, 1, \ldots$. Although $r(k)$ typically tends to 0 as $k \to \infty$, this convergence is so slow that $\sum r(k)$ is diverges for a long-range dependent process. Formally, the process A is said to be *long-range dependent* if $\sum_{k=0}^{\infty} r(k)$ is divergent.

A *fractional Brownian motion* $X \equiv \{X(t) : t \geq 0\}$, with $X(0) = 0$ and $\mathbb{E}X(t) = 0$ for all $t \geq 0$, is defined as a continuous Gaussian process whose covariance function is given by

$$Cov(X(s), X(t)) = \frac{1}{2}(s^{2H} + t^{2H} + (t-s)^{2H}) \qquad s < t$$

where H is the Hurst parameter. The increment process $\{X(k+1) - X(k) : k = 0, 1, 2, \ldots\}$ is also a Gaussian process called *fractional Gaussian noise* (FGN). Straight forward computations show that X

i. has stationary increments

ii. is self-similar

iii. is long-range dependent when $1/2 < H < 1$.

D D D D Since a Gaussian process is fully characterized by its covariance function, an FBM is *strictly self-similar*, that is, the finite dimensional distributions of $\{X(\alpha t) : t \geq 0\}$ and $\{\alpha^H X(t) : t \geq 0\}$ are identical for all $\alpha > 0$. The FBM X is said to be *antipersistent* if $0 < H < 1/2$ and *persistent* if $1/2 < H < 1$. We will illustrate the meanings of these terms on simulated traces in Section 5. The case $H = 1/2$ corresponds to a *Brownian motion*, which has independent increments.

We now specify A to be an FBM traffic (NORROS (1995)) given by

$$A(t) = mt + \sqrt{ma}X(t) \tag{1}$$

where X is a (normalized) FBM as above, m is the mean traffic input rate, and $a > 0$ is a variance coefficient called the *peakedness* parameter. The parameter implicit through X in (1) is the Hurst parameter H. Here, the process X is regarded as dimensionless. Then, the dimensions of m and a determine that of the total traffic $A(t)$ at time t. For example when A(t) is measured in bits, m and a have the dimension bits/(time-unit) and bits·(time-unit), respectively. Note that both long-range dependence and (second-order) self-similarity properties are inherited by A from X.

2.2 FBM Simulation Methods

Since the formal introduction of FBM by MANDELBROT and VAN NESS (1968), several simulation methods have been proposed. While some of these methods are fast enough, fastness compromises accuracy in most cases. In fact, it is hard to capture all aspects of FBM numerically due to its fractal character. The aim is, then, to simulate traces with controlled numerical errors as well as to maintain a fast algorithm.

The only exact method to simulate an FBM would be to generate a Gaussian vector $X(t_1), \ldots, X(t_n)$ through Cholesky decomposition of its covariance matrix. Clearly, this approach is impractical for large n due to its complexity and memory requirement.

An approximate, but very fast approach is the random midpoint displacement method (LAU et.al. (1995)). It works by subdividing an interval recursively and constructing the values of FBM at midpoints from the values at end points, taking $O(n)$ time. To ensure fastness the increments in the recursion are chosen independently, which is not true for an FBM except for $H = 0.5$, the case of Brownian motion. As a result, the observed values of H deviate from the targeted values, and self-similarity does not quite hold. This method is more suitable for qualitative than quantitative analysis.

The direct approximation of the integral representation of FBM by a finite sum has been studied in MANDELBROT and WALLIS (1969) as one of the earlier approaches. While this is in time domain, another method called Weirstrass-Mandelbrot algorithm approximates the spectral representation of the Gaussian process FBM (MEHRABI et.al. (1997)). Both methods can be classified under *aggregation methods* which include more recent and efficient algorithms. The idea is to form a sum of the relevant terms in time or frequency domain to get the realization $X(t)$, for each $t = t_1, \ldots, t_n$. The remaining methods we review are all in this class.

Among the faster methods are those that involve fast Fourier transform (FFT), which involves $O(n \log n)$ operations. Here, a random sequence is formed in the Fourier domain using a form of the spectral density of FGN, and then transformed by an inverse FFT to time domain to obtain an FGN. The drawback of these methods is that spectral density cannot be taken as exact since it is in the form of an infinite sum. Typically, only the low frequency approximation is considered to capture long-range dependence. PAXON (1997) proposes a better approximation to the power spectrum and studies the resulting traces

empirically. The theoretical impact of all the approximations of the method on the numerical errors is unknown. Then, it is hard to assess, for example, the discrepancy between the targeted and input values of H for $H > 0.70$ as it may be equally due to the estimation method or the algorithm itself.

Wavelet synthesis of FBM is a faster aggregation method as the wavelet transform involves only $O(n)$ operations. The most frequently used form of the method starts with the generation of wavelet coefficients corresponding to an orthonormal basis (WORNELL (1990)). A realization of FBM is then obtained by an inverse wavelet transform. Although the distribution of the coefficients is chosen to be exact, the correlation between them is ignored. This yields only an approximate correlation structure, which at most captures the low frequencies. More recently, SELLAN (1995) has proposed aggregation through a *fractional* wavelet basis. Both the approximations and the details of wavelet analysis are included in the final representation, and they carry the short-term and long-term correlation information, respectively. The fast implementation of this method is given in ABRY and SELLAN (1996). The numerical errors implicit in the method are due to the truncation of the (fractional) wavelet representation to a finite sum over the scales and translations.

A constructive approximation to FBM is considered in TAQQU et.al. (1997). Here, many sources, which can be identified with those of packet traffic are superimposed. Each source represents an independent replica of a renewal process with *on* and *off* periods corresponding to packet transmission or no transmission, respectively. Both periods have distributions with heavy tail such as a Pareto distribution. The amount of traffic at any time is found by an integration of the rate of input given by the total number of on sources at that time instant. The properly normalized and centered traffic (around its mean) becomes a persistent FBM in the limit as the number of sources tends to infinity and larger and larger time scales are considered. This approach is valuable for its physical interpretation of the mechanism of self-similarity observed in network traffic. Despite the fact that generation of self-similar traffic with this method is fast, only $O(n)$, the implementation of it as a synthesis method for FBM needs further study as indicated by the authors. The order of the two types of limit calls for attention, and especially the limit taken in the time scale can affect actual time of computation.

The algorithm we present in this paper is a fast and accurate aggregation method of $O(n)$. The construction with micropulses possesses the theoretical

properties of an FBM, and our analysis shows that it is possible to control the numerical errors that come from replacing infinite sums with their finite versions. Although they do not have physical meaning as sources, the micropulses can be considered as units of traffic with duration of Pareto like distribution similar to "on" periods in the on/off model. Yet, we show that the approximation of an infinitely long past is computationally negligible in our implementation in contrast to the limit taken in the time scale there. What is more, the micropulses approach can simulate both persistent and antipersistent FBM. We analyze both cases below for the sake of completeness, although long-range dependence is represented by a persistent FBM. From another point of view, each micropulse is a random translation and dilation of a deterministic pulse. In that sense, aggregation with micropulses is essentially a wavelet synthesis, but with superior qualities. First, one can choose a closed form expression for the pulse shape, in other words the wavelet, from a wide range of possibilities. Second, there is no step of filtering to obtain the coefficients as in SELLAN (1995). Finally, this approach captures the scaling phenomena inherent in the self-similar processes like the wavelet synthesis does.

3 Generation with Micropulses

For generating an FBM, CIOCZEK-GEORGES and MANDELBROT (1996) aggregate random pulses of various shapes in their model where the location of each pulse in time, as well as its height and width are all governed by a Poisson random measure. The approximating process at time t is defined as the sum of changes in the total pulse height between times 0 and t. Then, an FBM is obtained as a limit by the transformation of the pulses to micropulses while the number of them increases to infinity.

Specifically, let N_ϵ be a Poisson random measure on $\mathbb{R} \times \mathbb{R}_+$, where $\mathbb{R}_+ = (0, \infty)$, with mean measure

$$n_\epsilon(d\tau, dw) = \epsilon^2 w^{-\delta-1}\, d\tau dw \qquad\qquad t \in \mathbb{R}, w \in \mathbb{R}_+ \tag{2}$$

where $\epsilon > 0$ and $1 < \delta < 3$. The variables τ and w have the interpretations as the time of arrival and the width (or duration) of a pulse, respectively. Then, the expected number of pulses with arrival times in $[t_1, t_2]$ and widths in $[w_1, w_2]$ are found from (2) by

$$\int_{w_1}^{w_2} \int_{t_1}^{t_2} \epsilon^2 w^{-\delta-1}\, d\tau dw$$

for every $t_1, t_2 \in \mathbb{R}$ and $w_1, w_2 \in \mathbb{R}_+$.

Let f be a deterministic function with support $[0,1]$ representing a *pulse* shape. The difference in pulse height at time t and time 0 is defined as

$$g(t,\tau,w) = w\left[f\left(\frac{t-\tau}{w}\right) - f\left(\frac{-\tau}{w}\right)\right] \quad . \tag{3}$$

The height of the pulse will be rescaled by a factor $x \in \mathbb{R}$, which can be interpreted as the tangent of the base angle in conical pulses given in CIOCZEK-GEORGES and MANDELBROT (1996). Originally, x is random and is also governed by N_ϵ. However, we take it to be deterministic here for simplicity of notation and since it is not relevant for the results of the present paper. Further scaling of f by $\epsilon > 0$ yields a *micropulse* whose height decreases to zero as $\epsilon \to 0$. Then, adding up the micropulse differences corresponds to integration with respect to N_ϵ to give the approximating process

$$X_\epsilon(t) = \int_{\mathbb{R}\times\mathbb{R}_+} \epsilon x g(t,\tau,w)\, N_\epsilon(d\tau, dw) \; . \tag{4}$$

For clarification of the integral (4), we can rewrite it equivalently as the sum

$$X_\epsilon(t) = \sum_{(\tau_i, w_i)} \epsilon x g(t,\tau,w)$$

where (τ_i, w_i), $i = 1, 2, \ldots$, are the atoms of N_ϵ. We explain this construction further in the implementation phase in the next section. Note that, in view of (2), as $\epsilon \to 0$, the number of micropulses increases to infinity, and the construction of X_ϵ resembles a wavelet synthesis with the random translations and dilations of f through the pulse g.

Let X denote an FBM with parameter

$$H = (3-\delta)/2 \qquad 1 < \delta < 3,$$

and with variance $c\,x^2$ where

$$c = \int_{\mathbb{R}\times\mathbb{R}_+} g^2(1,\tau,w) w^{-\delta-1}\, d\tau dw \; . \tag{5}$$

When f is a Lipschitz continuous function with $f(0) = f(1) = 0$, we have

$$X_\epsilon \to X \qquad \text{as } \epsilon \to 0 \tag{6}$$

in the sense of finite dimensional distributions, by Proposition 3.1 of CIOCZEK-GEORGES and MANDELBROT (1996). The convergence is true for all $1 < \delta < 3$, or equivalently for all $0 < H < 1$. The result extends to more general Hölder continuous functions f on $[0,1]$, and the values of δ that ensure the convergence vary accordingly.

We observe that the process X_ϵ satisfies two properties of an FBM, namely stationarity of the increments and (second-order) self-similarity. They can both be checked through the characteristic function

$$\exp\left\{\int_{\mathbb{R}\times\mathbb{R}_+} (\mathrm{e}^{i\sum_{k=1}^n \xi_k \epsilon x g(t_k,\tau,w)} - 1)\, n_\epsilon(d\tau, dw)\right\} \tag{7}$$

of $X_\epsilon(t_1), \ldots, X_\epsilon(t_n)$ where $\xi_1, \ldots, \xi_n \in \mathbb{R}$. We can compute a similar expression for the characteristic function of the finite dimensional distributions of $\{X_\epsilon(t+s) - X_\epsilon(s) : t \geq 0\}$, for each $s \geq 0$, as

$$\exp\left\{\int_{\mathbb{R}_+}\int_{\mathbb{R}} (\mathrm{e}^{i\sum_{k=1}^n \xi_k \epsilon x w[f((t_k+s-\tau)/w) - f((s-\tau)/w)]} - 1)\, \epsilon^{-2} w^{-\delta-1}\, d\tau\, dw\right\} \quad .$$

Making a change of variable $\tau - s$ to τ shows that this expression is free of s. This being true for all $s > 0$ implies that the increments of X_ϵ are stationary.

The covariance function can be found by evaluating the derivatives of (7) at $\xi_1 = \ldots = \xi_n = 0$. It is given by

$$\mathrm{Cov}(X_\epsilon(t_k), X_\epsilon(t_j)) = \frac{c\, x^2}{2}\, (t_k^{3-\delta} + t_j^{3-\delta} - |t_k - t_j|^{3-\delta}) \, . \tag{8}$$

Note that the covariance is free of ϵ and is equal to that of an FBM even before the limit is taken. Hence, for each $\alpha > 0$, $X_\epsilon(\alpha t)$ and $\alpha^H X_\epsilon(t)$, $H = (3-\delta)/2$, have the same covariance structure. That is, X_ϵ is second-order self-similar. However, the limiting process X in Equation (6) is strictly self-similar. The long-range dependence property is satisfied when $1/2 < H < 1$, or $1 < \delta < 2$.

4 Implementation

Our purpose is to evaluate the approximation

$$X_\epsilon(t) = \int_{\mathbb{R}\times\mathbb{R}_+} \epsilon x g(t,\tau,w)\, N_\epsilon(d\tau, dw) \tag{9}$$

for each $\epsilon > 0$ as precisely as possible. This amounts to generating the atoms of N_ϵ for a particular choice of pulse shape. In implementation, two problems arise: the need for a cutoff parameter and a truncation parameter.

The need for a cutoff parameter becomes apparent from the mean measure (2); the steps of implementation are as follows. In order to obtain the atoms (τ_i, w_i), $i = 1, 2, \ldots$ of N_ϵ, we must first generate the arrival times $\tau_1, \tau_2, \ldots$ of a homogeneous Poisson process with rate

$$\lambda_0 = \epsilon^{-2} \int_{\mathbb{R}_+} w^{-\delta-1}\, dw$$

which is the expected number of arrivals in an infinitesimal interval of time $[\tau, \tau + d\tau]$. But, λ_0 does not have a finite value. This is also evident from the next step. We need to sample $w_1, w_2, \ldots$ as associated marks to $\tau_1, \tau_2, \ldots$ from the density

$$h(w) = w^{-\delta-1}\, dw$$

for $w > 0$, which cannot be made into a probability density since $\int_{\mathbb{R}_+} h(w)\, dw = \infty$. This difficulty arises because of the fractal nature of FBM as discussed in CIOCZEK-GEORGES and MANDELBROT (1995). Here, we tackle the problem by introducing a cutoff value to the Pareto density h, and evaluate the resulting numerical errors.

A truncation parameter is necessary because of the impossibility of generating an infinite past. In particular, we consider the conical pulse f

$$f(t) = \frac{1}{2} - |t - \frac{1}{2}| \qquad \text{if} \quad 0 \le t \le 1 \tag{10}$$

which is an isosceles triangle with base $[0, 1]$ and base angle $\pi/4$ as given in CIOCZEK-GEORGES and MANDELBROT (1996). Then, we get the difference

$$g(t, \tau, w) = (w/2 - |t - \tau - w/2|)1_{\{\tau \le t \le \tau + w\}} - (w/2 - |\tau + w/2|)1_{\{\tau \le 0 \le \tau + w\}} \tag{11}$$

in (9) where τ in fact has limits $(-\infty, t)$ rather than $\mathbb{R}$. We truncate this interval to (T, t), $T < 0$, and compute the associated numerical errors.

4.1 Cutoff for Pareto distribution

We generate $w_1, w_2, \ldots$ from a Pareto distribution with density

$$h(w) = \delta\, b^\delta\, w^{-\delta-1} \qquad\qquad w \ge b \tag{12}$$

where $b > 0$ is the cutoff parameter. We only change the address space $\mathbb{R} \times \mathbb{R}_+$ to $\mathbb{R} \times (b, \infty)$ at this stage, and keep the mean measure (2) the same. This affects the variance of the process X_ϵ.

The covariance of X_ϵ is computed by

$$\begin{aligned}
\text{Cov}\,(X_\epsilon(t_k), X_\epsilon(t_j)) &= x^2 \int_{\mathbb{R}} \int_b^\infty g(t_k, \tau, w) g(t_j, \tau, w) w^{-\delta-1}\, d\tau dw \\
&= \frac{x^2}{2} \left\{ \int_{\mathbb{R}} \int_b^\infty g^2(t_k, \tau, w) w^{-\delta-1}\, d\tau dw \right. \\
&\quad + \int_{\mathbb{R}} \int_b^\infty g^2(t_j, \tau, w) w^{-\delta-1} d\tau dw \\
&\quad \left. - \int_{\mathbb{R}} \int_b^\infty [g(t_k, \tau, w) - g(t_j, \tau, w)]^2\, w^{-\delta-1}\, d\tau dw \right\}
\end{aligned}$$

Similar to the analysis in CIOCZEK-GEORGES and MANDELBROT (1996), we make change of variables τ/t to τ, w/t to w in the first two integrals and make a change of variable τ to $(\tau - t_j)/|t_k - t_j|$ in the last integral. We get

$$\begin{aligned}
\text{Cov}\,(X_\epsilon(t_k), X_\epsilon(t_j)) &= \frac{x^2}{2} \left\{ t_k^{3-\delta} \int_{\mathbb{R}} \int_{b/t_k}^\infty g^2(1, \tau, w) w^{-\delta-1}\, d\tau dw \right. \\
&\quad + t_j^{3-\delta} \int_{\mathbb{R}} \int_{b/t_j}^\infty g^2(1, \tau, w) w^{-\delta-1} d\tau dw \\
&\quad \left. - |t_k - t_j|^{3-\delta} \int_{\mathbb{R}} \int_{b/|t_k - t_j|}^\infty g^2(1, \tau, w) w^{-\delta-1}\, d\tau dw \right\} \quad . \qquad (13)
\end{aligned}$$

In view of (5), note that

$$\int_{\mathbb{R}} \int_{b/t}^\infty g^2(1, \tau, w) w^{-\delta-1}\, d\tau dw = c - \int_{\mathbb{R}} \int_0^{b/t} g^2(1, \tau, w) w^{-\delta-1}\, d\tau dw\,.$$

For $t > b$, we compute with g of (11) that

$$\int_0^{b/t} g^2(1, \tau, w) w^{-\delta-1}\, d\tau dw = \frac{(b/t)^{3-\delta}}{6(3-\delta)}\,.$$

This quantity is larger if $t < b$, that is why we consider $t > b$, which will be taken into consideration in sampling. Then, from (13) for $t_k, t_j, |t_k - t_j| > b$, we have

$$\text{Cov}\,(X_\epsilon(t_k), X_\epsilon(t_j)) = \frac{c\, x^2}{2} \left(t_k^{3-\delta} + t_j^{3-\delta} - |t_k - t_j|^{3-\delta}\right) - \frac{x^2\, b^{3-\delta}}{12(3-\delta)} \qquad (14)$$

It is clear that second order self-similarity does not exactly hold with the introduction of the cutoff b, but its impact on the error is as computed in (14). Stationarity of the increments of X_ϵ as shown in Section 3 still holds. Another conclusion we draw from this analysis is that b determines the level of resolution as we chose $t_k, t_j, |t_k - t_j| > b$; that is, the sampling interval has to exceed b.

4.2 Choice of accuracy and the arrival rate

With the introduction of a cutoff value b, we will be able to generate a Poisson process with finite rate

$$\lambda = \epsilon^{-2} \int_b^\infty w^{-\delta-1}\, dw = \frac{\epsilon^{-2}}{\delta b^\delta}\ .$$

Once b is determined, the arrival rate will be controlled by the accuracy parameter ϵ in simulations.

The parameter λ is the total number of pulses with widths greater than b. We indeed generate sufficiently many of these, as required by the mean measure (2). For each $a > b$, the expected number of pulses in $[0,t] \times (a,\infty)$ is computed from (2) as

$$\epsilon^{-2} \int_a^\infty w^{-\delta-1}\, dw = \frac{\epsilon^{-2}}{\delta a^\delta}\, t\ \ . \tag{15}$$

On the other hand, in simulations we generate arrivals of a Poisson process N with rate λ, and associate $w_1, w_2, \ldots$ from the Pareto distribution (12) to them. The expected number of arrivals in $[0,t]$ with widths greater than $a > b$ is given by

$$\mathbb{E} \sum_{i=1}^{N(t)} 1_{\{W_i > a\}} = \mathbb{E}\, N(t)\, \mathbb{P}\{W > a\} = \frac{\epsilon^{-2}}{\delta b^\delta} t\, \frac{\delta b^\delta}{\delta a^\delta} = \frac{\epsilon^{-2}}{\delta a^\delta}\, t$$

by independence of the arrival times and the widths. This is exactly (15). As ϵ gets smaller, we have more arrivals in every interval (a,∞), $a > b$, as desired.

The arrival rate λ affects the number of pulses aggregated at each time, and is determined by ϵ once the cutoff b is set. Indeed, b determines self-similarity as it appears in (14), rather than the number of aggregated pulses. Then, ϵ is the parameter that determines Gaussianity as intended in the approximation model. As a rule of thumb, the marginals are practically Gaussian when the number of aggregated pulses is greater than 30 at each time.

4.3 Truncation of the past

In numerical simulations, we consider pulses that have arrived only after $T < 0$. As a result of this, the stationarity of the increments is only approximate. We quantify this approximation by finding a bound on the expectation of the error.

Let $X_\epsilon^T(t)$ denote the value of the truncated process at time t. Then, we have

$$\begin{aligned}
\mathbb{E}\,|X_\epsilon - X_\epsilon^T| &= \mathbb{E}\,|\int_{-\infty}^{T}\int_{\mathbb{R}_+} \epsilon x w[f(\frac{t-\tau}{w}) - f(\frac{-\tau}{w})]\,N_\epsilon(d\tau, dw)\,| \qquad (16)\\
&\leq \mathbb{E}\int_{-\infty}^{T}\int_{\mathbb{R}_+} \epsilon x w|f(\frac{t-\tau}{w}) - f(\frac{-\tau}{w})|\,N_\epsilon(d\tau, dw)\\
&= \int_{-\infty}^{T}\int_{\mathbb{R}_+} \epsilon^{-1} x w^{-\delta}|f(\frac{t-\tau}{w}) - f(\frac{-\tau}{w})|\;d\tau dw
\end{aligned}$$

Recalling that f is nonzero only on $[0,1]$, we evaluate the above integral in regions $\{(\tau,w) : 0 < (t-\tau)/w < 1, 0 < -\tau/w < 1, \tau < T\}$ and $\{(\tau,w) : 0 < -\tau/w < 1, (t-\tau)/w > 1, \tau < T\}$. Note that f of (10) is Lipschitz continuous with a corresponding constant 1, and $-f(-\tau/w) = f(1) - f(-\tau/w)$. Then, from (16) we get

$$\begin{aligned}
\mathbb{E}\,|X_\epsilon - X_\epsilon^T| &\leq \epsilon^{-1}x\left[\int_{-\infty}^{T}\int_{t-\tau}^{\infty} w^{-\delta}\,\frac{t}{w}\,dw\,d\tau + \int_{-\infty}^{T}\int_{-\tau}^{t-\tau} w^{-\delta}\left(1+\frac{t}{w}\right)\,dw\,d\tau\right]\\
&= \epsilon^{-1}x\left[\frac{t}{\delta(\delta-1)(t-T)^{\delta-1}} + \frac{t^2}{2\delta(t-T)^{\delta}}\right. \qquad (17)\\
&\qquad \left. + \frac{1}{\delta(\delta-1)(\delta-2)(-T)^{\delta-2}} + \frac{\delta t^2 - \delta^2 t^2 + 2\delta t T - 2T^2}{2\delta(\delta-1)(\delta-2)(t-T)^{\delta}}\right]
\end{aligned}$$

where we changed the order of integration for evaluation. As $T \to -\infty$, the expected error $\mathbb{E}\,|X_\epsilon - X_\epsilon^T|$ must go to 0 for all $0 < \delta < 1$. While showing this below, we also compute the slowest term. Writing the binomial series for $(t-T)^{d-1}$ and $(t-T)^d$, we get

$$\begin{aligned}
\frac{t}{\delta(\delta-1)(t-T)^{\delta-1}} &= \frac{t}{\delta(\delta-1)[T^{\delta-1} + \sum_{n=1}^{\infty}(\delta-1)\ldots(\delta-n)\,t^n(-T)^{\delta-1-n}/n!]}\\
&= \frac{t}{\delta(\delta-1)(-T)^{\delta-1}}\\
&\quad - \frac{t\sum_{n=1}^{\infty}(\delta-1)\ldots(\delta-n)\,t^n(-T)^{1-n}/n!}{\delta(\delta-1)[(-T)^{\delta} + \sum_{n=1}^{\infty}(\delta-1)\ldots(\delta-n)\,t^n(-T)^{\delta-n}/n!]}
\end{aligned}$$

$$= \frac{t}{\delta(\delta-1)(-T)^{\delta-1}} + \mathrm{O}\left((-T)^{-\delta}\right)$$

and similarly,

$$\begin{aligned}
\frac{2\delta t T}{2\delta(\delta-1)(\delta-2)(t-T)^{\delta}} &= -\frac{t}{(\delta-1)(\delta-2)(-T)^{\delta-1}} + \mathrm{O}\left((-T)^{-\delta}\right) \\
\frac{-2T^2}{2\delta(\delta-1)(\delta-2)(t-T)^{\delta}} &= -\frac{1}{\delta(\delta-1)(\delta-2)(-T)^{\delta-2}} + \frac{t}{(\delta-1)(\delta-2)(-T)^{\delta-1}} \\
&\qquad + \mathrm{O}\left((-T)^{-\delta}\right)
\end{aligned}$$

Putting all these in (17), we obtain

$$\mathbb{E}\,|X_\epsilon - X_\epsilon^T| \;\le\; \frac{x\,t}{\epsilon\,\delta\,(\delta-1)\,(-T)^{\delta-1}} + \mathrm{O}\left((-T)^{-\delta}\right). \tag{18}$$

The upper bound in (18) does not depend on the specific pulse shape we have chosen, and is valid for all Lipschitz continuous f with constant equal to 1 (generalization to Lipschitz constant M is obvious). The error increases as ϵ decreases; so one has to choose even bigger values of T in absolute value when sampling with higher accuracy. On the other hand, for lower values of δ close to 1, the impact of the magnitude of T on the error is stronger than that for higher values of δ. Low values of δ are equivalent to high values of H as $H = (3-\delta)/2$, which corresponds to persistent FBM. Indeed, for $1/2 < H < 1$ the expected number of pulses in distant past is a lot more than that for $0 < H < 1/2$, and this number is magnified by decreasing values of ϵ.

4.4 Algorithm and its complexity

In view of (11), the approximation (9) is equal to the difference of the sum of pulse heights at time t and that at time 0. So, at each time $t \ge 0$, we compute $X_\epsilon(t)$ as $Y_\epsilon(t) - Y_\epsilon(0)$ where

$$Y_\epsilon(t) = \sum_{T \le \tau_i \le t} \epsilon\, x\, (w_i/2 - |t - \tau_i - w_i/2|)\, 1_{\{\tau_i \le t \le \tau_i + w_i\}} \qquad t \ge 0\,. \tag{19}$$

The process Y_ϵ is finite because of the cutoff and the truncation parameters.

Note that a pulse arriving at $\tau < 0$ has impact on Y_0 only if its span w is greater than $-\tau$. So, it is sufficient to generate only the pulses (τ_i, w_i) with $w_i > -\tau_i$ when $\tau_i < 0$. This fact can be applied as follows. Divide the interval $[T, -1]$ into intervals of length Δt. The number of arrivals on $(T + (k-1)\Delta t, T + k\Delta t]$

that have widths greater than $a \equiv -(T + k\Delta t)$ is a Poisson random variable with mean

$$\Delta t\, \lambda_k = \Delta t\, \lambda\, \mathbb{P}\{W > a\} = \frac{\Delta t}{\epsilon^2 \delta b^\delta} \int_a^\infty \delta b^\delta w^{-\delta-1}\, dw = \frac{\Delta t}{\epsilon^2\, \delta\, a^\delta}\ .$$

Let W_k denote the width of such an arrival in $(T + (k-1)\Delta t, T + k\Delta t]$. For sampling purposes, we get the distribution of W_k by

$$\mathbb{P}\{W_k > w\} = \mathbb{P}\{W > w \,|\, W > a\} = \frac{\mathbb{P}\{W > w\}}{\mathbb{P}\{W > a\}} = \frac{(b/w)^\delta}{(b/a)^\delta} = (a/w)^\delta \qquad w > a\ .$$

So, W_k has a Pareto distribution like W, but with parameters a and δ.

The computational cost for the method is proportional to the total number of pulses generated. For $\Delta t > 0$, the number of pulses on $[T, -1]$ is given by

$$l \equiv \frac{\Delta t}{\delta\, \epsilon^2} \sum_{k=1}^{m} (-(T + k\Delta t))^{-\delta}$$

where $m = (-1 - T)/\Delta t$ is assumed to be an integer through the choice of Δt. We can approximate l by

$$l \approx \frac{1}{\delta\epsilon^2} \int_T^{-1} (-x)^{-\delta}\, dx = \frac{1}{\delta(\delta-1)\epsilon^2}(1 - (-T)^{1-\delta})$$

as $\Delta t \to 0$. The upper bound in (18) suggests the choice of

$$T \approx -(n/\epsilon)^{\frac{1}{\delta-1}}$$

when we evaluate $X_\epsilon(t)$ for $t \le n$. Therefore,

$$l \approx \frac{1}{\delta(\delta-1)\epsilon^2}(1 - \frac{\epsilon}{n})\ . \tag{20}$$

On the other hand, $\epsilon^{-2} b^{-\delta}/\delta$ arrivals need to be generated on $[-1, 0]$ as for each interval $[t-1, t]$, $t = 1, \ldots, n$. In view of this and (20), the total number of pulses generated is around $(n+2)\epsilon^{-2}$ for approximating $X_\epsilon(t)$ for $t = 1, \ldots, n$. Consequently, the total number of operations is $O(n)$.

The Poisson arrivals are generated through exponential interarrival times. The pulses are stored in the order they arrive in a data structure, which is updated frequently. Thus, the memory requirement remains stable around $\lambda\, \mathbb{E}W = \epsilon^{-2} b^{(1-\delta)}/(\delta - 1)$.

Suppose the desired variance parameter of FBM is $\alpha > 0$, that is,

$$Cov(X(t_1), X(t_2)) = \frac{\alpha}{2} \left(t_1^{3-\delta} + t_2^{3-\delta} - |t_1 - t_2|^{3-\delta} \right) .$$

Then, the steps to get $X_\epsilon(t)$ for $t = 1, \ldots, n$, with $n \sim (-T)^{\delta-1}$, are as follows.

1. Input $0 < \epsilon < 1$, $1 < \delta < 3$ ($\delta = 3 - 2H$), and $0 < b < 1$. Compute $x = \sqrt{\alpha/c}$.

2. Let $T_0 = T < T_1 < T_2 < \ldots < T_K = 0$ be a mesh of $[T, 0]$. In each interval $[T_{k-1}, T_k]$, $k = 1, \ldots, K$, generate Poisson arrivals with rate

$$\lambda_k = \frac{1}{\epsilon^2 \delta (-T_k)^\delta} .$$

   Associate widths w_i from the Pareto density (12) with cutoff $b = -T_k$.

   Repeat Step 3 for $t = 0, 1, \ldots, n$.

3. Compute $Y_\epsilon(t)$ by (19). Generate Poisson arrivals on $[t, t+1]$ with rate $\lambda = \epsilon^{-2} b^{-\delta}/\delta$. Associate widths from the Pareto density (12). Update the stack of pulses by adding the new arrivals and deleting the pulses that have $\tau_i + w_i < t + 1$.

4. $X_\epsilon(t) = Y_\epsilon(t) - Y_\epsilon(0)$, $t = 1, \ldots, n$.

5 Simulations

In this section, we first display sample traces of FBM. Then, several traces are simulated for statistical confirmation of the accuracy of the method with wavelet estimation. In particular, the estimator of the peakedness parameter is studied empirically.

Fractional Brownian motions for $H = 0.2, 0.5, 0.8$ are plotted in Figure 1 for $t = 0, 1, 2, \ldots,$ 1000. The value of T is -10^5 for $H = 0.2, 0.5$, and -10^{10} for $H = 0.8$. The value of ϵ is 0.1, which ensures that sufficiently many pulses are aggregated to achieve a Gaussian distribution. The variance α is chosen to be 1, and the value of b is such that $\delta b^\delta = 1$ which yields $0 < b < 1$. The corresponding fractional Gaussian noises are given in Figure 2 for $t = 1, 2, \ldots, 1000$. The effect

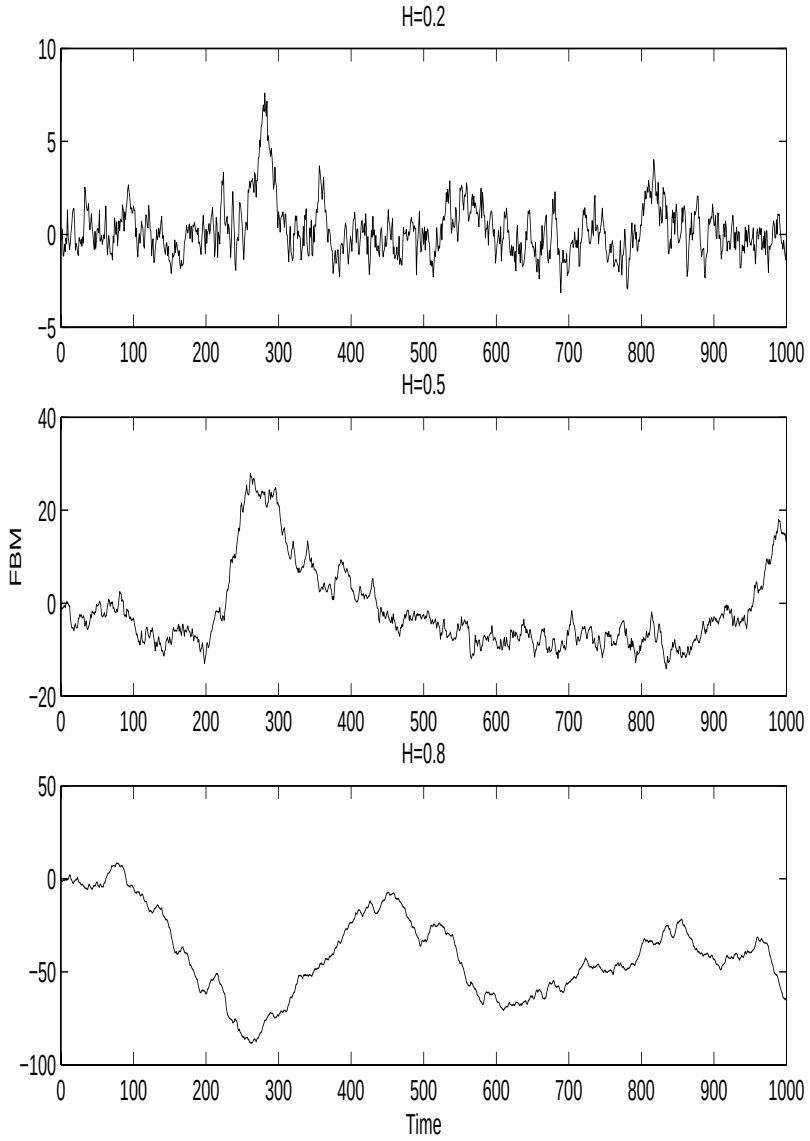

Figure 1: Standard Fractional Brownian motion for $H = 0.2, 0.5, 0.8$ from top to bottom.

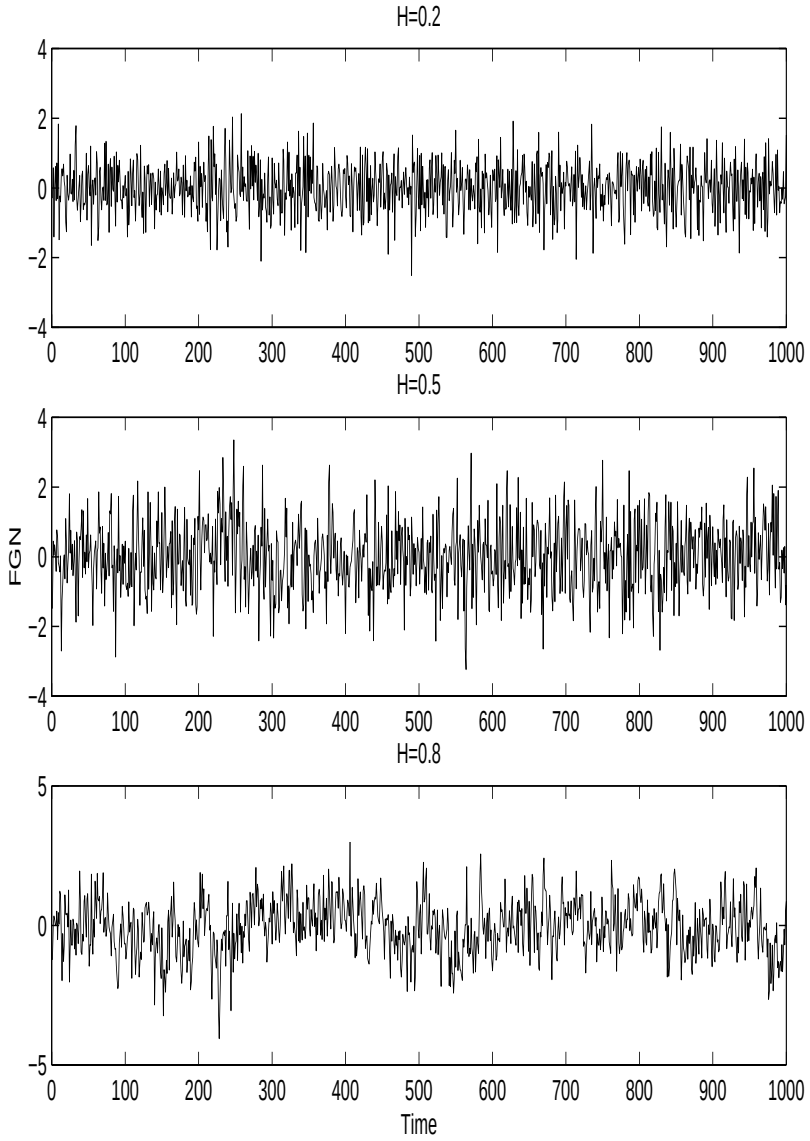

Figure 2: Standard Fractional Gaussian noise for $H = 0.2, 0.5, 0.8$ from top to bottom.

of $b < 1$ on the error of the variance α is small as we plot for t greater than or equal to 1.

It is well known that the qualitative difference between these graphs comes from the sign of the autocorrelation of the increments of FBM X in nonoverlapping intervals. We have, for each $h > 0$,

$$Cov(X(t+h)-X(t), X(t)-X(0)) = \mathbb{E}\left[X(t)(X(t+h)-X(t))\right] = \frac{1}{2}\left[(t+h)^{2H}-t^{2H}-h^{2H}\right]$$

which is positive for $H > 1/2$, negative for $H < 1/2$, and is zero for $H = 1/2$, corresponding to the persistent, antipersistent and independent cases, respectively. Indeed, the plots of FGN fluctuate less as H increases, which is consistent also with the FBM plots. For example for $H = 0.8$ in Figure 1, the process is inclined to increase (decrease) if it has already increased (decreased) in the previous interval. The rightness of the choice of ϵ, b and T can be checked from FGN plots qualitatively. Since these plots are over unit intervals, we are plotting Gaussian random variables with mean 0 and standard deviation 1 in all cases. Clearly, the differences are due to those of the autocorrelations.

To test the accuracy of the simulation procedure, we estimate the parameters $H \equiv (3-\delta)/2$ and $\alpha \equiv cx^2$ of (8) jointly by the wavelet estimation method of VEITCH and ABRY (1997). This method has proven to be quite precise for estimating the Hurst parameter; see for example FISCHER and AKAY (1996), and MEHRABI et.al. (1997) among others. The work of VEITCH and ABRY (1997) takes it one step further by jointly estimating a form of the scale parameter as well as the shape parameter in long-range dependent processes. The shape parameter they consider is a linear function of H in our case. The scale parameter they consider is denoted by c_f, which is the coefficient in

$$f(\nu) \sim c_f\,|\nu|^{-(2H-1)} \qquad \nu \to 0$$

where f is the spectrum of the stationary long-range dependent process, in our case FGN. Because of long-range dependence, their analysis refers to $H > 1/2$ for FGN, however it can be extended to $H \leq 1/2$ without loss of generality.

In the FBM traffic model of (1), we have

$$A(t) = mt + \sqrt{ma}X'(t) \tag{21}$$

where X' is a normalized FBM with $\alpha = 1$. In the simulated traces of this section, we have also set $\alpha = 1$. However, we treat α as an unknown in the

estimation process. Then one could take

$$X(t) \equiv \sqrt{ma}X'(t)$$

and hence

$$Var(X(t)) = \alpha t^{2H} = ma\, t^{2H} = ma\, Var(X'(t)) = Var(A(t))$$

Then, estimating α from a trace of X is equivalent to estimating "ma" from a trace of A as they are both the variance coefficients. This is in turn eqivalent to estimating the peakedness parameter a by $a = \alpha/m$ once the mean m is estimated. That is why, we estimate α to illustrate the estimation of a in (21) rather than c_f, as a directly appears in the traffic model, while c_f does not. Besides, when the micropulses algorithm is used for simulation of FBM, the input parameter is α not c_f. Then, the parameter α is given in terms of c_f by

$$\alpha = \frac{c_f\,(2\pi)^{2H-1}}{2\,,\,(2H-1)\cos((2H-1)\pi/2)(2H-1)H} \qquad H \neq \frac{1}{2}\,. \tag{22}$$

In the estimation process, there are two unbiased estimators, namely, those of H and $c_f C$ where C is the integral

$$C = \int |\nu|^{-(2H-1)}\,|\Psi_0(\nu)|^2\,d\nu \tag{23}$$

of the Fourier transform Ψ_0 of the mother wavelet. In particular, we use Daubechies wavelets with two vanishing moments. Under mild assumptions, which approximately hold in the case of FGN, the estimators $\hat{H}$ and $\widehat{c_f C}$ are both unbiased. Essentially, we estimate α through (22) using the estimators $\hat{c}_f$ and $\hat{H}$ where $\hat{c}_f = \widehat{c_f C}/\hat{C}$ and $\hat{C}$ is the integral (23) computed with $\hat{H}$. However, being an involved function of these estimators $\hat{\alpha}$ is not necessarily unbiased. It can be interpreted as the variance per time lag that the observations are separated, which is usually taken as the unit time 1. When the estimation is desired for another time unit, say γ times the time unit of the observations, the estimator $\hat{\alpha}$ must be written in full generality as

$$\hat{\alpha} = \frac{\hat{c}_f\,(2\pi)^{2\hat{H}-1}\,\gamma^{2\hat{H}}}{2\,,\,(2\hat{H}-1)\cos((2\hat{H}-1)\pi/2)(2\hat{H}-1)\hat{H}}\,. \tag{24}$$

This follows by the fact that $V(X_{t+\gamma} - X_t) = \alpha_1 \gamma^{2H}$ where $\alpha_1 = V(X_{t+1} - X_t)$ is the variance per the time unit of the observations.

For particular simulations in VEITCH and ABRY (1997), $\hat{H}$ and $\hat{c}_f$ perform well especially with samples of length at least 2^{12}. We have simulated 100 samples of FGN for each $H = 0.1, 0.2, \ldots, 0.9$, by setting $\alpha = 1$. In the preliminary trials, FGN was generated for 2^{13} time units, and b was such that $\delta b^\delta = 1$ so that the arrival rate was just ϵ^{-2}. This produced $0 < b < 1$ for all $1 < \delta < 3$ justifying the sampling at unit intervals. Here, the variance of $\hat{\alpha}$ appeared to be large for $H < 1/2$ although its bias was in an acceptable range. Decreasing b improved the results in view of Section 4.1. So, for $H \leq 1/2$, we choose $b = 0.3$, sample twice in each time unit for $n = 2^{12}$, yielding a sample size of 2^{13} in the estimation stage. For $H > 1/2$, b is such that $\delta b^\delta = 1$, and $n = 2^{13}$. The mean of the estimators of H as well as the approximate 95% confidence intervals are given in Figure 3. Since the estimator of H is unbiased theoretically, the results indicate that the aggregation method is accurate in terms of the shape parameter H. The means and confidence intervals for $\hat{\alpha}$ are given in Figure 4. In view of the time units, $\hat{\alpha}$ is found by setting $\gamma = 1$ for $H > 1/2$ and $\gamma = 2$ for $H \leq 1/2$ in (24). From Figure 4, we see that the estimator $\hat{\alpha}$ is either biased or the aggregation method produces samples of larger variance than we intended.

To reach a conclusion, we have also estimated $\widehat{c_f C}$, which is known to be unbiased. The true values of c_f are found by the equation

$$c_f = \frac{2\alpha\,,\,(2H-1)\cos((2H-1)\pi/2)(2H-1)H}{(2\pi)^{2H-1}\,\gamma^{2H}} \qquad H \neq \frac{1}{2}$$

which takes the desired time unit into account through γ. This consideration is done in the true value rather than $\hat{c}_f$, not to upset the unbiasedness of the estimator. For $H = 1/2$, $f(\nu) = c_f$ is a constant. Since the time unit is 0.5 for $H = 1/2$, we have $c_f = V(X_{t+0.5} - X_t) = 0.5$ and $c_f C = 0.5$ as $C = 1$. The confidence intervals on the estimator are found by normal approximation because this gives almost the same result as the lognormal distribution, which is the approximate distribution of $\widehat{c_f C}$. The true and estimated values of $c_f C$ together with approximate 95% confidence intervals are given in Figure 5. We see that for some H, $\widehat{c_f C}$ is very close to $c_f C$, and for others there is some error. Since the aggregation method is exactly the same for all H, the difference is due to the randomness in simulation. The bias is at most 20%, which we expect to decrease for longer samples. The variances, on the other hand, are directly proportional to the magnitude of $c_f C$, which is as expected from the theoretical variance given in VEITCH and ABRY (1997). Therefore, the aggregation method with micropulses is accurate in terms of the scale parameter as well.

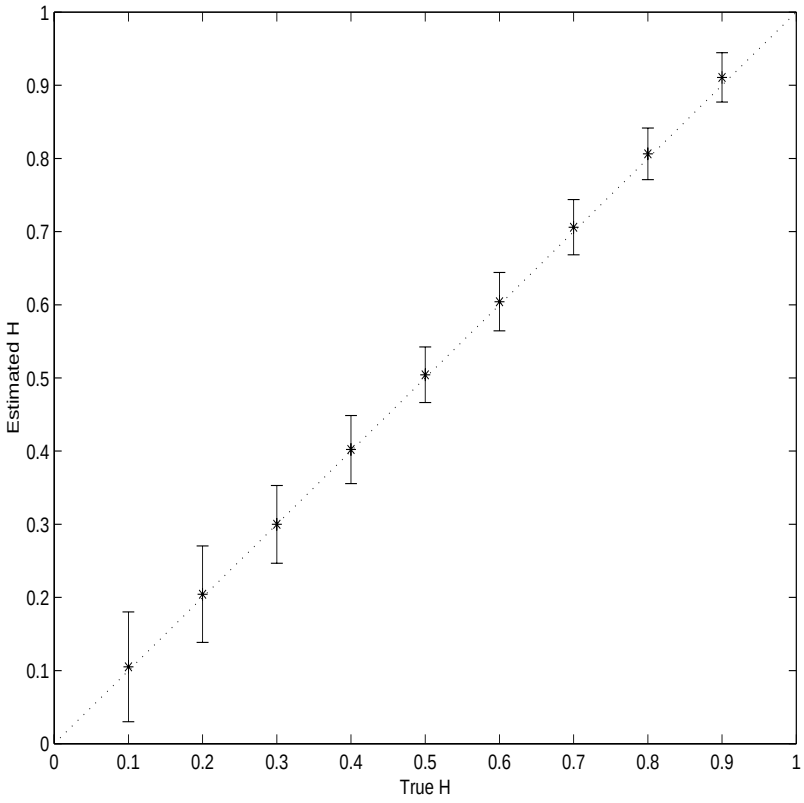

Figure 3: The mean and approximate 95% confidence intervals for H estimated from 100 samples of FGN for $H = 0.1, 0.2, \ldots, 0.9$. The dotted line is for reference.

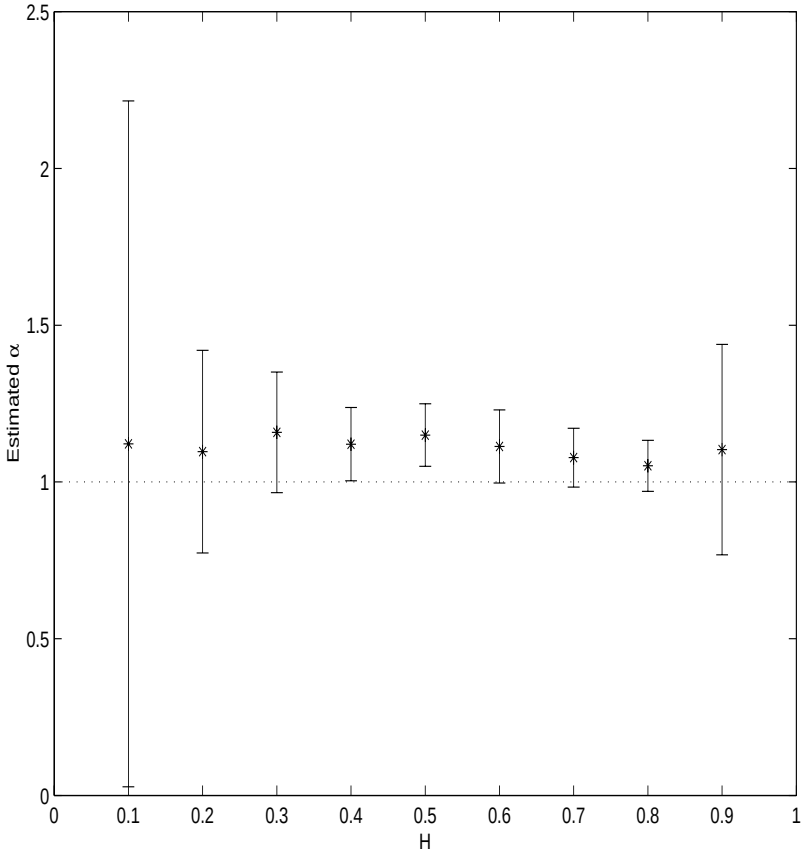

Figure 4: The mean and approximate 95% confidence intervals for α estimated from 100 samples of FGN for $H = 0.1, 0.2, \ldots, 0.9$. The dotted line is for reference as the true α is 1.

Finally, with confidence in the aggregation method with micropulses, we can interpret Figure 4 from estimation aspect. The variance of $\hat{\alpha}$ is huge for small H somewhat in accordance with that of the corresponding $c_f C$. It is larger than expected for small H and also for $H = 0.9$. The estimator $\hat{\alpha}$ could be slightly biased as it deviates from the true value, which is not even in the confidence interval for some H in our simulations. However, the error being less than 20% as in the unbiased estimator $\widehat{c_f C}$, with moderate variances for $H > 1/2$, this method of estimation of α would be useful for long-range dependence in telecommunication studies.

Acknowledgement. I would like to thank Dr. Iraj Saniee for introducing me to the traffic models with fractional Brownian motion. This work would not have been possible without his invaluable suggestions and comments.

REFERENCES

P. Abry and F. Sellan (1996) The Wavelet-Based Synthesis for Fractional Brownian Motion Proposed by F. Sellan and Y. Meyer: Remarks and Fast Implementation. *Appl. Comp. Harmonic Anal.* **3**: 377-383.

J. Beran et.al. (1995) Long-Range Dependence in Variable-Bit-Rate Video Traffic. *IEEE Trans. on Commun.* **43**: 1566-1579.

R. Cioczek-Georges and B.B. Mandelbrot (1995) A Class of Micropulses and Antipersistent Fractional Brownian Motion. *Stoch. Proc. Appl.* **60**: 1-18.

R. Cioczek-Georges and B.B. Mandelbrot (1996) Alternative Micropulses and Fractional Brownian Motion. *Stoch. Proc. Appl.* **64**: 143-152.

M. Crovella and A. Bestavros (1996) Self-Similarity in World Wide Web Traffic-Evidence and Possible Causes. *Proceedings of ACM Sigmetrics '96.* Philadelphia, PA, 160-169.

D.E. Duffy et.al. (1994) Statistical Analysis of CCSN/SS7 Traffic Data from Working Subnetworks. *IEEE J. Select. Areas Commun.* **12**: 544-551.

A. Erramilli et.al. (1996) Experimental Queuing Analysis with Long-Range Dependent Packet Traffic. *IEEE/ACM Trans. On Networking* **4**(2) : 209-223.

R. Fischer and M. Akay (1996) A Comparison of Analytical Methods for the Study of Fractional Brownian Motion. *Annals of Biomedical Engineering* **24**: 537-543.

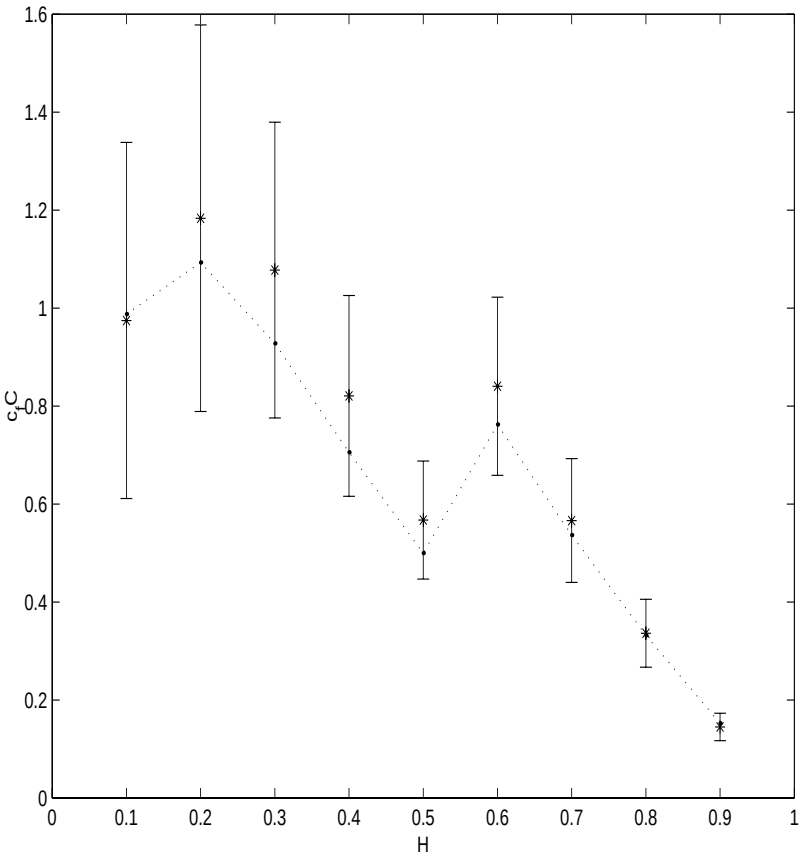

Figure 5: The mean and approximate 95% confidence intervals for $c_f C$ estimated from 100 samples of FGN for $H = 0.1, 0.2, \ldots, 0.9$. The dotted line joins the true values of $c_f C$.

H.J. Fowler and W.E. Leland (1991) Local Area Network Traffic Characteristic, with Implications for Broadband Network Congestion Management. *IEEE J. Select. Areas Commun.* **9**: 1139-1149.

D. Heath et.al. (1998) Heavy Tails and Long Range Dependence in On/Off Processes and Associated Fluid Models. *Mathematics of Operations Research* **23**: 145-165.

W.E. Leland et.al. (1994) On the Self-Similar Nature of Ethernet Traffic (extended version). *IEEE/ACM Trans. on Networking* **2**: 1-15.

W-C. Lau et.al. (1995) Self-Similar Traffic Generation: The Random Midpoint Displacement Algorithm and its Properties. IEEE International Conference on Communications. **1**: 466-472.

B.B. Mandelbrot and J.W. Van Ness (1968) Fractional Brownian Motions, Fractional Noises and Applications. *SIAM Review* **10**: 422-437.

B.B. Mandelbrot and J.R. Wallis (1969) Computer Experiments with Fractional Gaussian Noises. *Water Resources Research* **5**: 228-267.

A.R. Mehrabi, H. Rassamdana and M. Sahimi (1997) Characterization of Long-Range Correlations in Complex Distributions and Profiles. *Physical Review E* **56**: 712-722.

K. Meier-Hellstern et.al. (1991) Traffic Models for ISDN Data Users: Office Automation Application. *Proc. 13th ITC.* Denmark, 167-172.

I. Norros (1995) On the Use of Fractional Brownian Motion in the Theory of Connectionless Networks. *IEEE Jour. Selec. Areas in Comm.* **13**: 953-62.

V. Paxon and S. Floyd (1995) Wide-Area Traffic: The Failure of Poisson Modeling. *IEEE/ACM Trans. on Networking* **3**(3): 226-244.

V. Paxon (1997) Fast, Approximate Synthesis of Fractional Gaussian Noise for Generating Self-Similar Network Traffic. *Computer Communication Review* **27**(5): 5-18.

G. Samorodnitsky and M.S. Taqqu (1994) *Stable Non-Gaussian Random Processes.* Chapman & Hall. New York, NY.

F. Sellan (1995) Synthèse de Mouvements Browniens Fractionaires à l'aide de la Transformation par Ondelettes. *C. R. Acad. Sci. Paris Sér. I Math.* **321**: 351-358.

M.S. Taqqu, W. Willinger and R. Sherman (1997) Proof of a Fundamental Result in Self-Similar Traffic Modeling. *Computer Communication Review* **27**: 5-23.

G. Wornell (1990) A Karhunen-Loève like Expansion for 1/f Processes via

Wavelets. *IEEE Trans. Inform. Theory* **36**: 859-861.
D. Veitch and P. Abry (1997) A Wavelet Based Joint Estimator of the Parameters of Long-Range Dependence. Submitted to special issue "Multiscale Statistical Signal Analysis and its Applications" *IEEE Trans. Info. Th.*
Z.-M. Yin (1996) New Methods for Simulation of Fractional Brownian Motion. *Jour. of Comp. Phys.* **127**: 66-72.